

Structure–Function Analysis of RAMP1–RAMP3 Chimeras[†]

Tao Qi,^{||} John Simms,^{‡,§} Richard J. Bailey,^{||} Mark Wheatley,[⊥] Dan L. Rathbone,[‡] Debbie L. Hay,^{||} and David R. Poyner^{*,‡}

[‡]*School of Life and Health Sciences, Aston University, Birmingham B4 7ET, U.K.*, [§]*Department of Pharmacology, University of Monash, Clayton 3800, Australia*, ^{||}*School of Biological Sciences, University of Auckland, Auckland, New Zealand*, and [⊥]*School of Biosciences, University of Birmingham, Birmingham B15 2TT, U.K.*

Received November 6, 2009; Revised Manuscript Received December 17, 2009

ABSTRACT: The role of receptor activity modifying protein 1 (RAMP1) in forming receptors with the calcitonin receptor-like receptor (CLR) and the calcitonin receptor (CTR) was examined by producing chimeras between RAMP1 and RAMP3. RAMPs have three extracellular helices. Exchange of helix 1 of the RAMPs or residues 62–69 in helix 2 greatly reduced CLR trafficking (a marker for CLR association). Modeling suggests that these exchanges alter the CLR recognition site on RAMP1, which is more exposed than on RAMP3. Exchange of residues 86–89 of RAMP1 had no effect on the trafficking of CLR but reduced the potency of human (h) α CGRP and adrenomedullin. However, these alterations to RAMP1 had no effect on the potency of h β CGRP. These residues of RAMP1 lie at the junction of helix 3 and its connecting loop with helix 2. Modeling suggests that the loop is more exposed in RAMP1 than RAMP3; it may play an important role in peptide binding, either directly or indirectly. Exchange of residues 90–94 of RAMP1 caused a modest reduction in CLR expression and a 15-fold decrease in CGRP potency. It is unlikely that the decrease in expression is enough to explain the reduction in potency, and so these may have dual roles in recognizing CLR and CGRP. For CTR, only 6 out of 26 chimeras covering the extracellular part of RAMP1 did not reduce agonist potency. Thus the association of CTR with RAMP1 seems more sensitive to changes in RAMP1 structure induced by the chimeras than is CLR.

The receptor activity modifying proteins (RAMPs)¹ are a family of three single-pass membrane proteins that can associate with a number of G-protein coupled receptors (GPCRs) to modify their properties (1). They were initially identified as components of the receptors for calcitonin gene-related peptide (CGRP) and adrenomedullin (AM). They associate with the GPCR component of these receptors, calcitonin receptor-like receptor (CLR), trafficking both it and themselves to the cell surface. They also confer ligand binding on these complexes. CLR with RAMP1 produces the CGRP receptor with around 10-fold selectivity for CGRP over AM. By contrast, coexpression of CLR with RAMP2 or RAMP3 gives the AM₁ and AM₂ receptors. The AM₁ receptor has a very high selectivity for AM over CGRP; the AM₂ receptor will bind CGRP, albeit with about 50-fold lower potency than AM (2, 3).

RAMPs can interact with a range of other GPCRs (4); the best characterized of these is the calcitonin receptor (CTR). Unlike CLR, RAMP coexpression does not alter delivery of the CTR to the cell surface, at least in the cell lines examined to date.

However, the RAMPs alter the pharmacology of the CTR to produce receptors for amylin (AMY) (5, 6). The AMY_{1(a)} receptor formed from the CTR_(a) splice variant and RAMP1 has a higher affinity for CGRP than the AMY_{3(a)} receptor, formed from RAMP3 (6, 7).

While there is now considerable information about the pharmacology of RAMP complexes with both CLR and CTR, little is known about the structural basis underlying RAMP action. Early work used a series of deletions to identify possible functional domains in all three RAMPs (8, 9), although the interpretation of this work is not simple as the constructs are likely to have significant effects on overall protein folding. A significant development has been the publication of a crystal structure for the isolated N-terminus of human (h) RAMP1 (residues 27–107) (10). This has demonstrated that the protein is made of three helices, stabilized with three disulfide bonds. Evidence from both inspection of the crystal structure and mutagenesis has implicated Y66, F93, H97, and F101 of RAMP1 in CLR interactions (10, 11). These residues cluster together on the portion of RAMP1 which is probably nearest to the membrane. Above this is another cluster of residues; L69 and T73 have been implicated in CGRP binding by mutagenesis (11), and W74 is needed for the high-affinity binding of the CGRP antagonist BIBN4096BS (12). It has also been suggested that R67, D71, N78, and W84 of RAMP1 are likely to be involved as part of the same CGRP binding domain, but experimental evidence for this is currently lacking (10). These residues are all distributed on helices 2 and 3 and the interconnecting loops. Several studies of RAMP3 have been carried out (8, 13–16); these have indicated some functionally important residues or regions, but it is difficult to fully appreciate these data in the absence of a structure for this molecule.

[†]This work was supported by grants from the Biotechnology and Biological Sciences Research Council of the U.K. (C20090) to D.R.P. and M.W. D.L.H. was supported by the Auckland Medical Research Foundation, Maurice and Phyllis Paykel Trust, Health Research Council, and New Zealand Lottery Health Fund.

*To whom correspondence should be addressed. Tel: +44 (0)121 204 3997. Fax: +44 (0)121 359 5142. E-mail: D.R.Poyner@aston.ac.uk.

¹Abbreviations: AM, adrenomedullin; BIBN4096BS, *N*-[2-[[5-amino-1-[4-(4-pyridinyl)-1-piperazinyl]carbonyl]pentyl]amino]-1-[(3,5-dibromo-4-hydroxyphenyl)methyl]-2-oxoethyl]-4-(1,4-dihydro-2-oxo-3(2*H*)-quinazolinyl)-1-piperidinecarboxamide; CGRP, calcitonin gene-related peptide; CLR, calcitonin receptor-like receptor; rmsd, root mean square deviation; *E*_{max}, maximum response; GPCR, G-protein coupled receptor; h, human; HA, hemagglutinin; pEC₅₀, –log EC₅₀; RAMP, receptor activity modifying protein; TBS, Tris-buffered saline; WT, wild type.

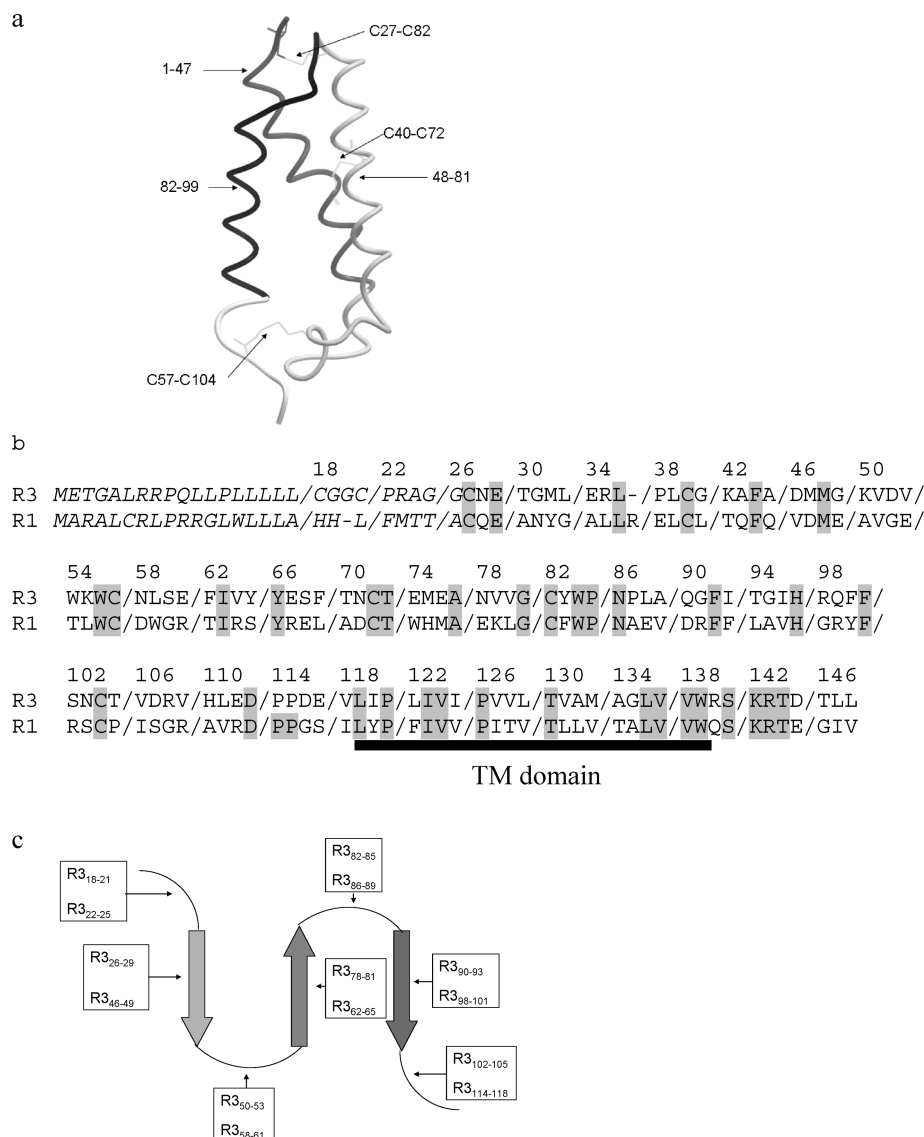


FIGURE 1: Chimera structures. (a) The regions sequentially exchanged in the large chimeras, shown for RAMP1. Their relationships with the disulfide bonds are illustrated. (b) The regions involved in the small chimeras. For each chimera, the block of four amino acids in RAMP1 was replaced by the corresponding amino acids in RAMP3. The putative signal peptides are shown in italics. Identical residues are shaded. The probable location of the transmembrane domain is shown by the solid black bar. (c) Schematic illustration of the location of the small chimeras along the three helices and interconnecting loops of the extracellular domain of RAMP1/3. Chimeras beyond R3_{114–118} are located in either the transmembrane or intracellular domains and are not shown.

In the current study, 32 chimeras between RAMP1 and RAMP3 have been produced to further probe the regions of these molecules that are responsible for the differences in pharmacology seen when they are complexed with CLR and CTR. RAMP1 and RAMP3 are of similar lengths, and both interact with AM and CGRP with reasonable, but markedly distinct, affinities (3); thus chimeras between the two are likely to be functional. The data have been interpreted using models for RAMP1 and RAMP3. This suggests that there are subtle but important differences in the structure of the CLR binding sites between the two RAMPs and that the N-terminal part of helix 3 and the adjacent loop to helix 2 are of particular importance in peptide binding and discrimination.

EXPERIMENTAL PROCEDURES

Materials. Human α CGRP, Tyr⁰-h α CGRP, rat amylin (rAmy), and hAM were from Bachem (Bubendorf, Switzerland). h β CGRP was from Bachem or American Peptide (Sunnyvale, CA). Peptides were dissolved in distilled water and stored as

aliquots at -20°C in siliconized microcentrifuge tubes (Bio Plas). Unless otherwise specified, chemicals were from Sigma (St. Louis, MO). Cell culture reagents were from Invitrogen (Carlsbad, CA). Forskolin was from Tocris (Ellisville, MO).

Expression Constructs and Mutagenesis. Human CLR with an N-terminal hemagglutinin (HA) epitope tag (HA-CLR) and h RAMP3 and h RAMP1 with or without an N-terminal myc epitope tag (mycRAMP1) were provided by Dr. S. M. Foord (GlaxoWellcome, Stevenage, U.K.). HA-tagged human CTR_(a) was the leucine polymorphic variant (17). Mutagenesis was carried out using the QuikChange site-directed mutagenesis kit (Stratagene, Cambridge, U.K.), following the manufacturer's instructions. Forward and reverse oligonucleotide primers were designed with multiple base changes to incorporate amino acid mutations, and the length of the oligonucleotides was altered to maintain the overall melting temperature of the primer. The primers were synthesized by Invitrogen. The locations of the chimeras are shown in Figure 1.

Plasmid DNA was extracted from the cultures using a Wizard-Prep DNA extraction kit according to the manufacturer's instructions (Promega, Southampton, U.K.). The plasmid DNA was eluted in 100 μ L of sterile distilled water and stored at -20°C . Sequences were confirmed by sequencing (Functional Genomics, Birmingham, U.K.).

Cell Culture and Transfection. Culture of Cos-7 cells was described previously; these do not express endogenous CLR, CTR, or RAMPs (18). Cells were cultured in Dulbecco's modified Eagle's medium (DMEM) containing $\sim 8\%$ heat-inactivated fetal bovine serum (FBS) and 5% (v/v) penicillin/streptomycin. Cells were plated into 96-well plates 1 day prior to transfection with polyethylenimine (PEI) as described (18). For preparation of cell lysates for Western blotting, cells were plated into six-well plates and transfected with a total of 5 μ g of DNA per well.

Assay of cAMP Production. Growth medium was removed from the cells and replaced with DMEM containing 1 mM isobutylmethylxanthine and 0.1% BSA for 30 min. Peptide agonists in the range 1 pM to 1 μ M were added for a further 15 min. Ice-cold ethanol (95–100% v/v) was used to extract cAMP, which was subsequently measured by radio-receptor assay in a 96-well plate as previously described (18).

Analysis of Cell-Surface Expression of Mutants by ELISA. Cell-surface expression of mutant receptor complexes was measured as previously described (19). Briefly, cells were fixed and washed in phosphate-buffered saline (PBS) prior to incubation in 0.6% hydrogen peroxide in PBS and blocked in 10% goat serum (in PBS) for 1 h. Cells were incubated with anti-HA.11 monoclonal primary antibody (Covance; MMS-101P, 1:2000 in PBS with 1% goat serum) for 30 min at 37°C . Horseradish peroxidase-linked anti-mouse secondary antibody (Amersham; NA931-1 ML, 1:500 in PBS with 1% goat serum) was added after washing and incubated at room temperature for 1 h. Substrate (SIGMAFAST OPD (Sigma)) was added and incubated for 15 min in the dark. The reaction was terminated with 0.5 M H_2SO_4 ; plates were read at 490 and 650 nm. Cresyl violet stain was added for 30 min, the wells were washed once, and 1% SDS was added for 1 h. The absorbance at 595 nm was determined, and the $(A_{490} - A_{650})/A_{595}$ was calculated for each well. Values were background-corrected and normalized to wild-type HA-CLR/RAMP1 expression levels.

Analysis of Total Cellular Expression of Mutants by Western Blotting. Total expression of selected small RAMP1/RAMP3 chimeras was measured as previously described with some modifications (11). Briefly, cell lysates were harvested from cells grown in six-well plates, and protein concentrations were estimated using Quick Start Bradford Dye Reagent 1X protein measurement assay (Bio-Rad). Proteins in cell lysate preparations were denatured and then separated in a NuPAGE 4–12% Bis-Tris precast gel system (Invitrogen) (20 μ g of proteins was applied to the first gel while 15 μ g of proteins was applied to the second and third gels). Proteins were transferred onto iBlot gel transfer stacks polyvinylidene fluoride (PVDF) membrane (Invitrogen) using the iBlot dry blotting system (Invitrogen). Blots were then blocked with 5% milk in Tris-buffered saline (TBS, pH 7.4) containing 0.1% Tween 20 (TBS-T) for 1 h at room temperature and incubated overnight at 4°C with a 1:400 dilution of primary anti-c-myc mouse mAb (9E10; Calbiochem), and an antibody specific for glyceraldehyde-3-phosphate dehydrogenase (GAPDH) at a dilution of 1:200000 (Abcam, 6C5, AB8245) was prepared in TBS-T containing 2.5% milk. After three washes the next day, blots were incubated for 1 h at room

temperature with a 1:2000 dilution of secondary Ecl sheep anti-mouse horseradish peroxidase linked antibody (as ELISA) prepared in 5% milk in TBS-T. Blots were washed and developed with an ECL Plus Western blotting detection system (Amersham) for 5 min, and the chemiluminescent signal was detected using a LAS3000 imaging system (Fujifilm). Protein bands were analyzed densitometrically with Multi Gauge software v2.2 (Fujifilm). The intensity of each single band detected with the anti-c-myc antibody was normalized to the intensity of corresponding GAPDH band from the same lane to account for possible differences in protein loading. Normalized protein band intensities were expressed as a percentage of the WT mycRAMP1/HA-CLR control sample intensities. Three independent transfections were performed for each mutant and WT and run on independent gels.

Molecular Modeling. A homology model for hRAMP3_{28–107} was produced by submitting the sequence to the Swiss-model server (<http://swissmodel.expasy.org/SWISS-MODEL.html>) using the crystal structure for the equivalent portion of hRAMP1 (PDB 2YX8) as a template. The structure was subjected to energy minimization and subsequent MD simulation using the Sander module with the ff99 Amber force field (20) within the Amber 9 package (21). The protein was neutralized with sodium counterions in a truncated octahedral box of TIP3P water (22) extending at least 8 Å out from the protein. The nonbonded cutoff distance was set to 12 Å. The ensemble was relaxed for 2000 steps of minimization and then heated from 0 to 300 K at constant volume periodic boundaries over 20 ps. Thereafter, the dynamics were conducted at 300 K and a constant pressure of 1 atm for at least 5 ns. Plots of the energy of RAMPs 1 and 3 vs time are given (Supporting Information Figures S1 and S2), and these indicate the systems became stable within 100 ps. Coordinates were saved at 0.5 ns intervals using the program VMD (23). Residue accessibility was analyzed using Swiss PDBviewer.

Data Analysis. Curve fitting was done with PRISM 4 or 5 (Graphpad Software Inc., San Diego, CA). For cyclic AMP studies, the data from each concentration–response curve were fitted to a sigmoidal curve to obtain the maximum response (E_{max}) and $-\log \text{EC}_{50}$ (pEC_{50}). For experiments with CLR using the small chimeras, the E_{max} was expressed as a percentage of maximum response to CGRP or AM as appropriate. For the remaining experiments, data were normalized to the 50 μ M forskolin control which was included in each experiment. A control WT experiment was included in every experiment. pEC_{50} and E_{max} values were compared by an unpaired Student's *t* test or by one-way ANOVA (with repeated measures as appropriate) followed by Dunnett's test. Total protein expression was analyzed by one-way ANOVA.

RESULTS

Modeling of hRAMP1 and hRAMP3. The homology model of RAMP3 is described elsewhere (24). In order to allow comparisons with RAMP1, it was necessary to subject the crystal structure of the latter to a molecular dynamics simulation in water. The resulting molecule was very similar to the parent crystal structure (root mean square deviation (rmsd) 1.91 Å); the differences were chiefly due to changes in the backbone of the last C-terminal three amino acids, beyond the final disulfide bond. The RAMP1 and RAMP3 models were superimposed (Figure 2). The overall rmsd between the C α atoms of the two

structures was 2.76 Å. The chief differences were with helices 1 (which was significantly unwound in RAMP3 compared to RAMP1), the loop between helices 2 and 3, and the orientation of the C-terminal portion of helix 3 (due to a kink in the helix in RAMP3). This alters the relative orientation of the residues believed to be important for CLR association; Y66, F93 (isoleucine in RAMP3), H97, and F101 are all more buried in RAMP3 than in RAMP1.

Effects of Large RAMP1/3 Chimeras Coexpressed with CLR. As an initial screen, the extracellular domain of RAMP1 was divided into three roughly equally sized portions, corres-

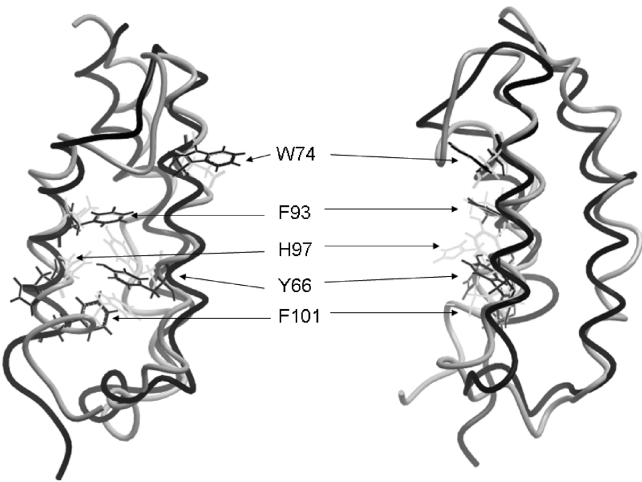







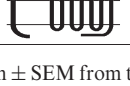


FIGURE 2: Comparison of the structures of RAMP1 and RAMP3: RAMP1, black; RAMP3, gray; left, view facing helices 2 and 3; right, view facing helices 1 and 2. The residues shown are likely to be involved in CLR binding; in addition, residue 74 (important for antagonist binding) is also shown.

ponding approximately to the three helices, and each was sequentially replaced by the corresponding section of RAMP3. The reciprocal chimeras were also constructed (Figure 1a). The ability of the chimeras to traffic CLR to the cell surface was measured (Table 1). As CLR is only poorly expressed at the cell surface in the absence of RAMPs, this provides a measure of the ability of the RAMPs to associate with this receptor, although it cannot distinguish between chimeras that are expressed by the cell but which do not recognize CLR and those that are misfolded and rapidly degraded. The ability of the chimera/CLR complex to respond to hαCGRP and AM was also measured (Table 1); if RAMP/CLR expression is normal, a reduction in peptide potency would suggest impaired ability of the ligand to either bind or activate the receptor. The controls behaved as expected (2, 3); hαCGRP was around 1300-fold more potent on CLR/RAMP1 than CLR/RAMP3 and AM was 25-fold more potent on CLR/RAMP1 (Table 1). It should be noted that in all the tables pEC₅₀ values are quoted; thus for CGRP the EC₅₀ of CLR/RAMP1 was 0.045 nM compared to 59 nM on CLR/RAMP3.

Substitution of the N-terminal section of RAMP1 by RAMP3 (RAMP3₁₋₄₇RAMP1₄₈₋₁₄₈) virtually abolished cell-surface expression of CLR; there was a smaller effect on the expression with the corresponding RAMP1₁₋₄₇RAMP3₄₈₋₁₄₈ chimera (Table 1). Otherwise, the expression of the chimeras was comparable to the parent RAMPs. Unsurprisingly, RAMP3₁₋₄₇RAMP1₄₈₋₁₄₈ failed to respond to either peptide, in line with the failure of the receptor complex to express at the cell surface. The reciprocal chimera RAMP1₁₋₄₇RAMP3₄₈₋₁₄₈ showed a reduced maximum response to both CGRP (58.5 ± 4.6% of CLR/RAMP1, *n* = 3) and AM (64% ± 4.9%, *n* = 3). Otherwise, all of the chimeras gave *E*_{max} values not significantly different from controls (data not shown). RAMP1₁₋₄₇RAMP3₄₈₋₁₄₈ also showed a lower pEC₅₀

Table 1: Expression and Potency of hαCGRP and hAM at Large RAMP1/RAMP3 Chimeras Coexpressed with CLR^a

Construct		pEC ₅₀ , hαCGRP	pEC ₅₀ , hAM	Expression
	RAMP1 ₁₋₁₄₈	10.35±0.15	8.51±0.17	100
	RAMP3 ₁₋₁₄₈	7.23±0.09***	9.90±0.15***	117.8±18.1
	RAMP1 ₁₋₄₇ RAMP3 ₄₈₋₁₄₈	6.54±0.28***	9.63±0.23*	74.5±6.34
	RAMP1 ₁₋₈₁ RAMP3 ₈₂₋₁₄₈	7.37±0.08***	8.05±0.49 ^{(a)(a)(a)}	109.6±6.08
	RAMP1 ₁₋₉₉ RAMP3 ₁₀₀₋₁₄₈	8.39±0.07***, ^{(a)(a)(a)}	8.72±0.24 ^(a)	140.5±3.05
	RAMP3 ₁₋₄₇ RAMP1 ₄₈₋₁₄₈	No response	No response	27.6±1.97**
	RAMP3 ₁₋₈₁ RAMP1 ₈₂₋₁₄₈	8.40±0.17***, ^{(a)(a)(a)}	9.29±0.13	94.5±5.73
	RAMP3 ₁₋₉₉ RAMP1 ₁₀₀₋₁₄₈	7.79±0.31***	9.62±0.20*	99.1±19.5

^aValues are mean ± SEM from three to six determinations. Expression is as a % of that seen with RAMP1 and CLR. The expression of CLR alone was 29.4 ± 3.94% (*n* = 6). ***, *P* < 0.001; **, *P* < 0.01; or *, *P* < 0.05 vs RAMP1; ^{(a)(a)(a)}, *P* < 0.001; ^{(a)(a)}, *P* < 0.01; or ^(a), *P* < 0.05 vs RAMP3; one-way ANOVA (Tukey's test).

than any other chimera when challenged with CGRP, but it responded to AM with a similar pEC_{50} as the parent RAMP3. As more of the RAMP1 sequence was introduced into RAMP3, the potency of CGRP increased and that of AM decreased. However, the potency of CGRP at RAMP1_{1–99}RAMP3_{100–148} was still not as high as at wild-type RAMP1. By contrast both RAMP1_{1–81}RAMP3_{82–148} and RAMP1_{1–99}RAMP3_{100–148} had AM potencies that were similar to that for RAMP1. For the RAMP1-based chimeras, there was a trend for the potency of AM to increase and for CGRP to decrease as more of the RAMP3 sequence was introduced; the potency of both AM and CGRP at RAMP3_{1–99}RAMP1_{100–148} was not significantly different from that at wild-type RAMP3 (Table 1).

Effects of Small RAMP1/3 Chimeras Coexpressed with CLR. To further delineate functional domains within RAMP1, a series of chimeras were produced where four amino acids at a time from RAMP3 were introduced into RAMP1 (Figure 1b,c). For convenience, a shortened form of nomenclature will be adopted in the text, based on the residues replaced. Thus the chimera where residues 18–21 of RAMP1 have been replaced by those of RAMP3 will be called R3_{18–21}. The chimeras were coexpressed with CLR. Their ability to traffic CLR to the cell surface was measured along with their ability to respond to hαCGRP (Table 2, Figures 3 and 4).

The chimeras R3_{22–25}, R3_{38–41}, and R3_{62–65} all failed to enhance CLR cell-surface expression above that seen in the absence of any added RAMP (Table 2). R3_{90–93} caused a 40% reduction in cell-surface expression. R3_{54–57}, R3_{66–69}, R3_{78–81}, and R3_{98–101} showed small reductions in cell-surface expression of around 1/3 (Table 2). All of the chimeras that had badly disrupted expression (including R3_{90–93}) also had significant reductions in pEC_{50} values (Table 2, Figure 3). However, while R3_{54–57} showed a significant reduction in pEC_{50} , the values for R3_{66–69}, R3_{78–81}, and R3_{98–101} were not significantly different from WT. R3_{86–89} had a reduced potency for hαCGRP despite showing normal expression. For all chimeras, the E_{max} was not significantly different from that observed with WT (data not shown) except for R3_{38–41}, where it was reduced by 72.5 ± 5.7%, consistent with a lack of substantial cell-surface expression. Chimeras R3_{22–25}, R3_{38–41}, R3_{62–65}, and R3_{90–93} showed the largest reductions in cell-surface expression. The exchanged region in chimera R3_{22–25} resides within the predicted signal peptide of RAMPs, which may explain the large reduction in cell-surface expression seen with this mutant. Therefore, total cellular expression was examined for the other three chimeras, R3_{38–41}, R3_{62–65}, and R3_{90–93}, by Western blotting (Figure 5). All chimeras were produced at the expected molecular weights, and there was no significant difference in expression with any of the chimeras compared to WT. The data suggest that the mutations introduced had no significant impact on intracellular synthesis of the proteins.

As R3_{86–89} gave a clear reduction in hαCGRP potency without any change in cell-surface expression, its pharmacology was further characterized with hβCGRP and hAM (Figure 4). Unlike with hαCGRP, there was no reduction in potency with hβCGRP (pEC_{50} WT 10.9 ± 0.16; pEC_{50} mutant 10.7 ± 0.04, $n = 4$). Also surprisingly, the hAM potency at this chimera was reduced almost 12-fold (pEC_{50} WT, 8.69 ± 0.16; pEC_{50} mutant, 7.63 ± 0.06, $n = 4$). The reciprocal RAMP3 mutant with the native residues in region 86–89 replaced by the corresponding residues in RAMP1 was in addition made and studied (R1_{86–89}). Unlike R3_{86–89}, R1_{86–89} showed responses not significantly different

Table 2: Expression and Potency of hαCGRP at Small RAMP1/RAMP3 Chimeras Coexpressed with CLR^a

construct	pEC_{50} WT	pEC_{50} mutant	expression
RAMP3 _{18–21}	10.3 ± 0.08	10.1 ± 0.19	105.1 ± 8.27
RAMP3 _{22–25}	9.93 ± 0.36	9.21 ± 0.51*	35.8 ± 11.9***
RAMP3 _{26–29}	9.62 ± 0.09	9.75 ± 0.08	74.5 ± 6.87
RAMP3 _{30–33}	9.62 ± 0.09	9.56 ± 0.08	72.1 ± 6.25
RAMP3 _{34–37}	10.1 ± 0.18	9.70 ± 0.13	86.3 ± 8.47
RAMP3 _{38–41}	9.68 ± 0.32	8.31 ± 0.32*	39.3 ± 6.22***
RAMP3 _{42–45}	9.80 ± 0.15	9.86 ± 0.19	79.2 ± 3.41
RAMP3 _{46–49}	9.97 ± 0.23	9.85 ± 0.11	73.3 ± 8.0
RAMP3 _{50–53}	9.83 ± 0.31	9.67 ± 0.21	88.7 ± 1.21
RAMP3 _{54–57}	9.62 ± 0.35	8.84 ± 0.71**	80.7 ± 5.05**
RAMP3 _{58–61}	9.59 ± 0.42	9.23 ± 0.36	87.1 ± 2.07
RAMP3 _{62–65}	9.92 ± 0.50	9.25 ± 0.52*	24.0 ± 3.03***
RAMP3 _{66–69}	9.92 ± 0.50	9.50 ± 0.50	66.7 ± 2.18***
RAMP3 _{70–73}	9.92 ± 0.50	9.50 ± 0.65	97.6 ± 4.81
RAMP3 _{74–77}	9.84 ± 0.65	9.80 ± 0.70	104.1 ± 0.98
RAMP3 _{78–81}	9.84 ± 0.65	9.87 ± 0.66	74.0 ± 3.68***
RAMP3 _{82–85}	9.84 ± 0.65	9.61 ± 1.00	88.8 ± 7.40
RAMP3 _{86–89}	10.2 ± 0.04	9.42 ± 0.10*	82.7 ± 4.49
RAMP3 _{90–93}	10.2 ± 0.04	9.07 ± 0.54*	60.9 ± 6.89***
RAMP3 _{94–97}	10.2 ± 0.04	10.2 ± 0.15	91.0 ± 5.47
RAMP3 _{98–101}	10.2 ± 0.04	9.97 ± 0.07	71.9 ± 1.90**
RAMP3 _{102–105}	10.4 ± 0.10	9.98 ± 0.08	95.7 ± 4.26
RAMP3 _{106–109}	10.4 ± 0.10	9.72 ± 0.27	79.0 ± 5.30
RAMP3 _{110–113}	10.4 ± 0.10	9.75 ± 0.14	93.2 ± 7.41
RAMP3 _{114–117}	10.4 ± 0.10	10.1 ± 0.04	89.6 ± 5.01
RAMP3 _{118–121}	10.4 ± 0.10	10.2 ± 0.08	87.2 ± 3.70
RAMP3 _{122–125}	10.3 ± 0.15	10.2 ± 0.12	ND
RAMP3 _{126–129}	10.3 ± 0.15	10.1 ± 0.16	ND
RAMP3 _{130–133}	10.3 ± 0.15	10.1 ± 0.15	ND
RAMP3 _{134–137}	10.0 ± 0.04	9.77 ± 0.27	ND
RAMP3 _{138–141}	10.0 ± 0.04	9.84 ± 0.29	ND
RAMP3 _{142–145}	10.0 ± 0.04	9.64 ± 0.29	ND
RAMP3 _{146–148}	9.74 ± 0.20	10.0 ± 0.29	ND

^aFor each entry, the construct indicates the residues of RAMP3 which were used to replace the corresponding residues of RAMP1. Values are mean ± SEM from three to six determinations. Expression is as a % of that seen with RAMP1 and CLR; the expression of CLR alone was 29.4 ± 3.94% ($n = 6$). ***, $P < 0.001$; **, $P < 0.01$; *, $P < 0.05$ vs WT; repeated means one-way ANOVA (cAMP) or one-way ANOVA (ELISA) (Dunnett's test). ND, not determined.

from WT controls for all three agonists tested (hαCGRP, pEC_{50} WT, 6.81 ± 0.15; pEC_{50} mutant, 6.85 ± 0.12, $n = 3$; hβCGRP, WT, 7.61 ± 0.25; pEC_{50} mutant, 7.93 ± 0.14, $n = 3$; and hAM, WT, 9.73 ± 0.12; pEC_{50} mutant, 9.75 ± 0.13, $n = 4$).

Effect of Chimeras Coexpressed with CTR_(a). To compare the role of RAMP1 in defining the pharmacology of another receptor, the large and small chimeras were also coexpressed with CTR_(a) to generate AMY receptors. RAMP1/CTR_(a) (AMY_{1(a)}) and RAMP3/CTR_(a) (AMY_{3(a)}) receptors may be pharmacologically differentiated using Tyr⁰-hαCGRP and hβCGRP; both activate AMY_{1(a)} receptors more potently than AMY_{3(a)} receptors (7). Therefore, the RAMP chimeras have the potential to provide insights into the molecular basis for this difference in pharmacology. As CTR is efficiently expressed at the cell surface in the absence of RAMPs, where it functions as a calcitonin receptor, it was not possible to measure RAMP chimera-CTR association. CTR expression was not quantified; as equal amounts of cDNA were transfected in all cells, it was assumed that this would not vary between treatment groups.

The AMY_{1(a)} receptor showed a 19-fold selectivity for hβCGRP and a 35-fold selectivity for Tyr⁰-hαCGRP over the

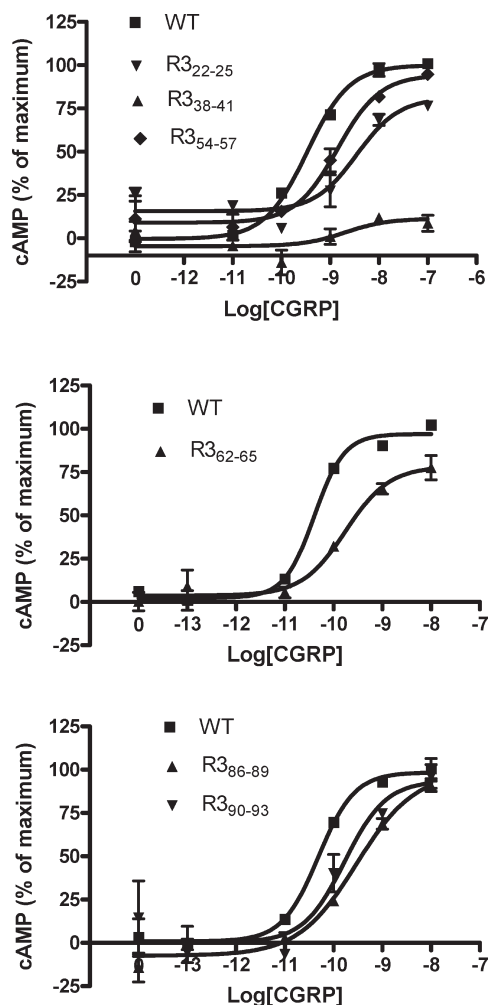


FIGURE 3: $h\alpha$ CGRP-stimulated cAMP response of the small RAMP1/RAMP3 chimeras. Cos-7 cells were transfected with CLR and WT RAMP1 or mutant RAMP1 and assayed for CGRP-stimulated cAMP production. WT and chimeric receptors are as indicated. Data are representative of three to six similar experiments. Points are mean \pm SEM of duplicate determinations.

AMY_{3(a)} receptor. Both agonists had weak potency at the CTR in the absence of any RAMP (Table 3). This is in agreement with values reported earlier (7, 14). For the chimeras based on RAMP3, replacement of the RAMP3 sequence with that of RAMP1 up to position 82 gave receptors that essentially had an AMY_{3(a)} pharmacology. However, substitution of the additional residues 82–99 with those from RAMP1 gave receptors that had a pharmacology not significantly different from that of the AMY_{1(a)} receptor (Table 3). For the chimeras based on RAMP1, RAMP3_{1–47}RAMP1_{48–148} gave receptors that were identical to CTR receptors. Given the fact that this chimera could not associate with CLR, it seems very likely that it could not also associate with CTR. The next chimera in the series, RAMP3_{1–81}RAMP1_{82–148}, showed a pharmacology that was essentially that of the AMY_{3(a)} receptor. However, the final chimera, RAMP3_{1–99}RAMP1_{100–148}, showed a complicated pharmacological profile. For Tyr⁰- $h\alpha$ CGRP the receptor resembled that for CTR alone. However, the potency of $h\beta$ CGRP was significantly different from that seen at CTR (Table 3), suggesting that there was association between the chimera and the CTR.

The majority of the small chimeras produced a significant decrease in the potency of $h\beta$ CGRP and Tyr⁰- $h\alpha$ CGRP

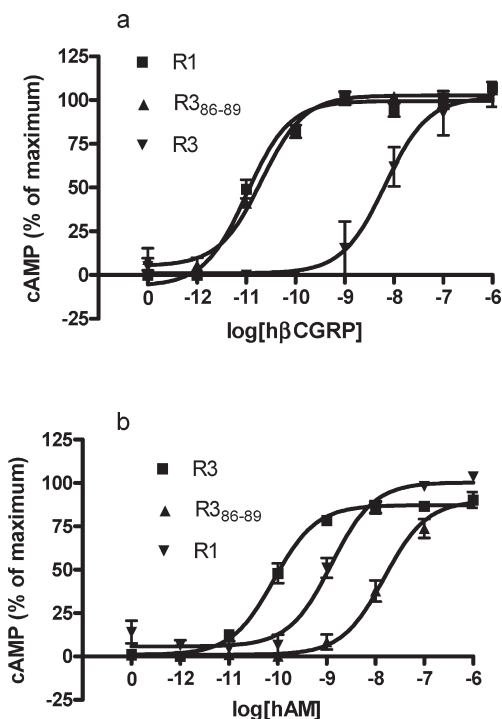


FIGURE 4: Agonist-stimulated cAMP response of R3_{86–89} coexpressed with CLR. Cos-7 cells were transfected with CLR and WT RAMP1, WT RAMP3, or mutant RAMP1 and assayed for cAMP production following challenge with $h\beta$ CGRP (a) or hAM (b). Data are representative of three to four similar experiments. Points are mean \pm SEM of triplicate determinations.

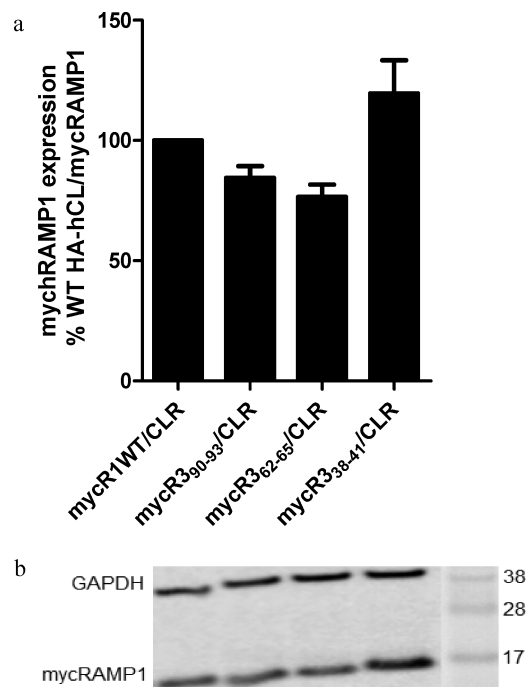


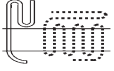
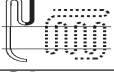


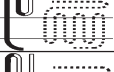

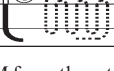


FIGURE 5: Effects of three RAMP1/RAMP3 chimeras on total cellular expression of mycRAMP1. (a) Mean expression obtained from quantitative Western blotting, $n = 3$ independent transfections and corresponding Western blots. Data were analyzed by one-way ANOVA followed by Dunnett's test vs WT; significance was achieved at $P < 0.05$. Significance was not achieved by any of the mutants. (b) Representative Western blot; order of lanes as bars in (a).

(Table 4). Indeed, only the chimeras R3_{18–21}, R3_{26–29}, R3_{42–45}, and R3_{70–73} and those from residue 106 onward did not reduce

Table 3: Potency of h β CGRP and Tyr⁰-h α CGRP at Large RAMP1/RAMP3 Chimeras Coexpressed with CTR^a

Construct	pEC ₅₀ , h β CGRP	pEC ₅₀ , Tyr ⁰ -h α CGRP
 CTR _(a) (No RAMP)	7.69±0.38 ^{@,*,**}	6.49±0.22 ^{*,@,@@}
 AMY _{1(a)} (RAMP1)	10.9±0.12 ^{@,@,++}	9.45±0.13 ^{++,@,@@}
 AMY _{3(a)} (RAMP3)	9.65±0.17 ^{*,*,++}	7.90±0.13 ^{*,*,++}
 RAMP1 ₁₋₄₇ RAMP3 ₄₈₋₁₄₈	8.91±0.18 ^{*,*,++,@}	7.26±0.12 ^{*,*,+,@}
 RAMP1 ₁₋₈₁ RAMP3 ₈₂₋₁₄₈	9.28±0.14 ^{*,*,++}	7.53±0.12 ^{*,*,++}
 RAMP1 ₁₋₉₉ RAMP3 ₁₀₀₋₁₄₈	10.4±0.12 ^{++,@}	8.94±0.08 ^{@,@,++}
 RAMP3 ₁₋₄₇ RAMP1 ₄₈₋₁₄₈	8.44±0.07 ^{*,*,@,@@}	7.01±0.17 ^{*,*,@,@@}
 RAMP3 ₁₋₈₁ RAMP1 ₈₂₋₁₄₈	9.18±0.16 ^{*,*,++}	7.54±0.12 ^{*,*,++}
 RAMP3 ₁₋₉₉ RAMP1 ₁₀₀₋₁₄₈	8.61±0.08 ^{*,*,+,@,@@}	6.98±0.15 ^{*,*,@,@@}

^aValues are mean ± SEM from three to four determinations. ++, $P < 0.01$; +, $P < 0.05$ vs CTR_(a); **, $P < 0.01$; *, $P < 0.05$ vs AMY_{1(a)}; @@, $P < 0.01$; @, $P < 0.05$ vs AMY_{3(a)}; unpaired t test.

the potency of one or other of the agonists. There were marked differences in the size of the reductions. R3₂₂₋₂₅, all the chimeras from R3₃₀₋₃₃ to R3₃₈₋₄₁, R3₆₂₋₆₅, R3₈₆₋₈₉, and R3₉₀₋₉₃ showed over a 100-fold decrease in potency of both agonists; R3₄₆₋₄₉, R3₅₄₋₅₇, and R3₆₆₋₆₉ showed a 30–100-fold decrease (for R3₅₄₋₅₇ this effect was only this large for Tyr⁰-h α CGRP). For most of these chimeras (those covering residues 22–25, 30–41, 46–49, 62–65, and 90–93), the responses to both agonists were the same as if they were acting at the CTR alone. R3₅₀₋₅₃, R3₇₈₋₈₁, and R3₉₄₋₁₀₁ showed a 10–30-fold decrease in potency for Tyr⁰-h α CGRP, although the difference was usually smaller for h β CGRP. For R3₁₁₈₋₁₂₁, the potency for both agonists was increased, although this was only significant for Tyr⁰-h α CGRP. Overall, there was a good correlation between the potency of the two agonists. There were few differences in the maximum responses of the chimeras. However, the three chimeras covering the region 50–61 all had a significantly decreased E_{\max} when challenged with Tyr⁰-h α CGRP (R3₅₀₋₅₃, $84 \pm 1.8\%$ of WT; R3₅₄₋₅₇, $70.6 \pm 1.7\%$ of WT; R3₅₈₋₆₁, $84 \pm 2.3\%$ of WT). Decreases were also seen with chimeras R3₆₆₋₆₉ ($84 \pm 2.6\%$ of WT), R3₇₄₋₇₇ ($81.5 \pm 3.1\%$ of WT), R3₇₈₋₈₁ ($77 \pm 1.3\%$ of WT), and R3₁₁₄₋₁₁₈ ($89 \pm 2.0\%$ of WT). Interestingly, these effects were not seen with h β CGRP, where the E_{\max} values were all similar to WT and there were no significant differences. R3₈₆₋₈₉ showed a significant $21 \pm 3.5\%$ increase in E_{\max} in response to h β CGRP whereas for Tyr⁰-h α CGRP there was a nonsignificant 3.5% decrease. The E_{\max} values for all other chimeras were not significantly different from WT.

A number of chimeras which showed a range of responses to h β CGRP or Tyr⁰-h α CGRP were tested for their ability to respond to rAmy. There were no changes in E_{\max} for any chimera. The chimeras that showed modest or no changes in response to the CGRP forms (R3₄₂₋₄₅, R3₅₈₋₆₀, R3₇₀₋₇₃) were not significantly different to WT AMY_{1(a)} in terms of rAmy potency. R3₅₀₋₅₃ and

R3₈₆₋₈₉ (medium and large changes in potency to CGRP forms) also had reduced rAmy potency (WT, 10.3 ± 0.12 ($n = 3$); R3₅₀₋₅₃, 9.69 ± 0.08 ($p < 0.05$ vs WT by t test, $n = 3$); R3₈₆₋₈₉, 8.99 ± 0.02 ($p < 0.001$ vs WT by t test, $n = 3$)). However, R3₉₄₋₉₇, which had a similar potency decrease to the CGRP forms as R3₅₀₋₅₃, had a WT AMY_{1(a)} response to rAmy.

DISCUSSION

This study provides new information about the structure–activity relationship for RAMP1 and RAMP3 and the way in which they interact with both GPCRs and peptide ligands. Overall, the results are consistent with a model in which the binding site for CGRP is formed by elements from both RAMP1 and CLR. The potential role of the different RAMP components are considered below.

The Role of Helix 1 with CLR. The data presented in this study suggest that helix 1 plays little direct role in interactions with either CLR or ligands. Instead, it maintains the overall structure of the molecule. This is consistent with the crystal structure (10). Chimeras involving the first 47 amino acids of either RAMP1 or RAMP3 (which include helix 1) showed either reduced or no association with either CLR or CTR. Given that the CLR recognition site is probably formed by residues from helices 2 and 3 (8–11), the simplest explanation of the results is that, in the chimeras, the introduced helix 1 causes distortion of the overall fold of the RAMP to make it nonfunctional.

The RAMP3 model predicts that helix 1 contains a stretch that is less tightly wound than in RAMP1 (perhaps due to the proline in RAMP3 at position 38). The formation of the disulfide bond between C40 and C72 may be compromised; the one small chimera in helix 1 that abolished CLR trafficking substituted residues 38–41.

The Roles of Helix 2 and Its Connecting Loops with CLR. The study suggested that helix 2 influences ligand recognition,

Table 4: Potency of hβCGRP and Tyr⁰-hαCGRP at Small RAMP1/RAMP3 Chimeras Coexpressed with CTR^a

construct	Tyr ⁰ -hαCGRP		hβCGRP	
	pEC ₅₀ WT	pEC ₅₀ mutant	pEC ₅₀ WT	pEC ₅₀ mutant
RAMP3 _{18–21}	8.61 ± 0.08	8.44 ± 0.06 ⁺	10.7 ± 0.24	10.60 ± 0.20 ⁺
RAMP3 _{22–25}	8.67 ± 0.07	6.61 ± 0.09***	10.6 ± 0.22	8.09 ± 0.19***
RAMP3 _{26–29}	8.72 ± 0.07	7.75 ± 0.49	10.5 ± 0.28	9.61 ± 0.26 ⁺
RAMP3 _{30–33}	8.67 ± 0.11	6.34 ± 0.12***	9.95 ± 0.42	7.81 ± 0.04**
RAMP3 _{34–37}	8.78 ± 0.10	6.61 ± 0.09***	10.7 ± 0.19	8.00 ± 0.20***
RAMP3 _{38–41}	8.60 ± 0.06	5.97 ± 0.24***	10.3 ± 0.28	7.82 ± 0.15***
RAMP3 _{42–45}	8.78 ± 0.13	8.17 ± 0.36 ⁺	10.5 ± 0.46	9.94 ± 0.38 ⁺
RAMP3 _{46–49}	8.56 ± 0.06	7.01 ± 0.19***	10.4 ± 0.34	8.47 ± 0.23**
RAMP3 _{50–53}	9.23 ± 0.04	8.16 ± 0.10***, +	10.5 ± 0.07	9.78 ± 0.21*, +
RAMP3 _{54–57}	9.23 ± 0.04	7.75 ± 0.10***, +	10.6 ± 0.09	9.60 ± 0.07***, +
RAMP3 _{58–61}	9.30 ± 0.04	8.50 ± 0.13***, +	10.5 ± 0.03	9.94 ± 0.15*, +
RAMP3 _{62–65}	9.12 ± 0.06	6.82 ± 0.15***	10.5 ± 0.03	8.42 ± 0.11***
RAMP3 _{66–69}	9.26 ± 0.01	7.40 ± 0.21***	10.6 ± 0.09	9.01 ± 0.19***, +
RAMP3 _{70–73}	9.27 ± 0.01	9.48 ± 0.16 ⁺	10.6 ± 0.13	10.94 ± 0.02 ⁺
RAMP3 _{74–77}	9.27 ± 0.01	8.49 ± 0.24*, +	10.4 ± 0.03	10.11 ± 0.19 ⁺
RAMP3 _{78–81}	9.27 ± 0.01	8.08 ± 0.04***, +	10.4 ± 0.03	9.58 ± 0.16***, +
RAMP3 _{82–85}	9.46 ± 0.11	8.66 ± 0.24*, +	11.4 ± 0.14	10.05 ± 0.53 ⁺
RAMP3 _{86–89}	9.60 ± 0.03	7.28 ± 0.03***	11.2 ± 0.20	8.66 ± 0.11***, +
RAMP3 _{90–93}	9.55 ± 0.08	6.98 ± 0.05***	11.4 ± 0.14	8.30 ± 0.11***
RAMP3 _{94–97}	9.46 ± 0.11	8.41 ± 0.26***, +	11.4 ± 0.14	10.41 ± 0.07***, +
RAMP3 _{98–101}	9.55 ± 0.08	8.44 ± 0.23*, +	11.4 ± 0.14	10.35 ± 0.06***, +
RAMP3 _{102–105}	9.55 ± 0.08	8.99 ± 0.18*, +	11.4 ± 0.14	10.61 ± 0.03***, +
RAMP3 _{106–109}	9.37 ± 0.13	8.60 ± 0.35 ⁺	11.1 ± 0.17	10.56 ± 0.24 ⁺
RAMP3 _{110–113}	9.29 ± 0.14	9.18 ± 0.31 ⁺	10.9 ± 0.17	10.68 ± 0.19 ⁺
RAMP3 _{114–117}	9.49 ± 0.07	9.21 ± 0.27 ⁺	11.1 ± 0.17	10.75 ± 0.22 ⁺
RAMP3 _{118–121}	9.51 ± 0.06	9.960 ± 0.12*, +	10.9 ± 0.19	11.07 ± 0.10 ⁺

^aFor each entry, the construct indicates the residues of RAMP3 which were used to replace the corresponding residues of RAMP1. Values are mean ± SEM from three or five determinations. ***, $P < 0.001$; **, $P < 0.01$; *, $P < 0.05$ vs AMY_{1(a)} receptor by *t* test; ⁺, $P < 0.05$ vs CTR; one-way ANOVA (Dunnett's test).

either directly or because of effects on CLR recognition. Residues at the N-terminal end of helix 2 were important for CLR recognition, with some also influencing CGRP binding. Helix 2 in RAMP3 was required for WT-like AM potency.

The largest effect on RAMP1 trafficking (and by implication, CLR recognition) was shown by the chimera involving residues 62–69, at the base of helix 2 (Table 2). This region includes Y66, which is important for CLR interaction in RAMP1; the residues are also close to the part of helix 3 which are probably involved in CLR interactions (11). The models of RAMP1 and RAMP3 predict that Y66 becomes more buried in RAMP3. The RAMP3 sequence inserted in the chimera, F⁶²IVY⁶⁵, is significantly more hydrophobic than the TIRS sequence in RAMP1 it replaces. This is a key part of RAMP structure, and it is possible that the residues in this region form an epitope crucial for overall RAMP stability. A smaller effect on trafficking was observed with residues 54–58, part of the loop connecting helices 1 and 2 (Figure 6). The small chimera covering this region also reduced CGRP potency. The reduced potency may involve more than the slight decrease in CLR surface expression as it is little different from that seen with other chimeras such as R3_{66–69} which have no effect on potency. The residues may have a dual role; by interacting with CLR, they alter its conformation so it is able to interact with CGRP.

The proximal end of helix 2 and the start of the connecting loop to helix 3 are also important for CLR association as judged by the effects of the chimera R3_{78–81}, although there is no obvious mechanistic explanation for this at this time.

The Role of Helix 3 with CLR. Helix 3, particularly at its junction with helix 2, is important for the binding of αCGRP and

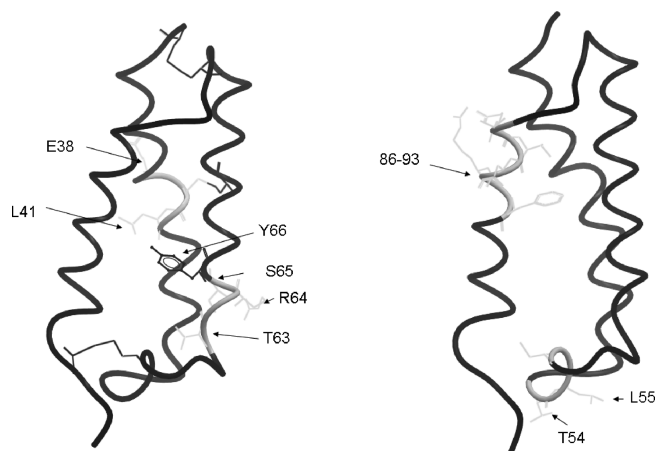


FIGURE 6: Areas of RAMP1 important for cell-surface expression of CLR (a) and αCGRP responsiveness when coexpressed with CLR (b). Regions discussed in the text are shown in light gray. Residues that are different between RAMP1 and RAMP3 are shown in stick formation. The disulfide bonds are in black as is Y66.

AM. Exchange of residues 86–89 reduced the potency of both of these agonists without affecting cell-surface expression. The residues in this chimera face T73 on helix 2, previously shown to be important for CGRP binding (11); they also border on the cluster of residues suggested by Kusano and colleagues to be important for CGRP binding based on the RAMP1 crystal structure (10) (Figure 5). Comparison of the models suggests that the upper part of helix 3 and the loop connecting it with helix 2 are more exposed in RAMP1 than in RAMP3 (Figure 2). Since

both AM and h α CGRP had reduced potency at this chimera, it suggests that the loop adopts a conformation found in neither of the parent molecules. As point mutations in this region do not give the same phenotype (14), there may be multiple contacts between these residues and the peptides or the effects are due to backbone interactions between this part of RAMP and the agonists.

Interestingly, the potency of h β CGRP was unchanged at this chimera. There are only three amino acid differences between h α CGRP and h β CGRP. That at position 3 is probably irrelevant as it is most likely to interact with the juxtamembrane domain of CLR, leaving those at positions 22 (valine in h α CGRP, methionine in h β CGRP) and 25 (asparagine in h α CGRP, serine in h β CGRP) to account for the differential binding. It is likely that this part of CGRP is somewhere in the vicinity of residues 86–89 of RAMP1 when it binds. The reciprocal chimera in RAMP3 failed to reduce potency of any of these agonists. As the loops in our RAMP1 and RAMP3 models are positioned differently, this may explain the data. It is predicted that CGRP and AM bind in a pocket formed from both CLR and RAMP; therefore, changes to RAMP structure may also influence the structure of the overall complex, thus influencing ligand binding.

The adjacent chimera, involving residues 90–93 toward the middle of helix 3, caused a small reduction in CLR surface expression and also CGRP potency. F93, within this chimera, can either reduce CLR association (11) or CGRP potency depending on how it is mutated (14). It appears to be another example of a residue that is involved in both processes.

The Role of the Juxtamembrane Region with CLR. RAMP1 has regions that are important for CGRP recognition beyond the end of helix 3. Alanine substitutions in this region can reduce CGRP potency (11), and the chimera RAMP1_{1–99}-RAMP3_{100–148} further supports these results. This gave a receptor with reduced potency for CGRP. As the reciprocal chimera, RAMP3_{1–99}-RAMP1_{100–148} behaved as full-length RAMP3 with regard to AM potency, this suggests that the juxtamembrane domain in RAMP3 makes a lesser contribution to ligand selectivity.

The Structure–Activity Relationship of RAMPs 1 and 3 with CTR. It is clear that despite the relatively high affinity of the AMY_{1(a)} receptor for CGRP and the homology between CLR and CTR, there are significant differences in the structure–activity relationship for RAMP1 in this complex. It was far more sensitive to changes induced by chimeras. The labile phenotype of the AMY_{1(a)} receptor is consistent with a less robust interaction between CTR with RAMP1 compared to CLR. Even in the presence of RAMP1, there is expression of uncomplexed CTR (6). The chimeras that produced a greater than 30-fold decrease in potency for agonists probably had a greatly impaired interaction with CTR. They include most of the chimeras that impaired cell-surface delivery of CLR. They lie in a diagonal stripe across the helix 2/3 interface (Figure 7). Their mechanism of action is likely to be the same as for CLR; they introduce distortions into the receptor recognition site on RAMP1. It is possible that this covers a wider area for CTR than is seen with CLR, but the alternative is that the interactions are intrinsically weaker and so more sensitive to disruption.

The experiments with the AMY_{1(a)} receptor also provided further support for the idea that each ligand interacts with the receptor in a subtly different way. Tyr⁰-h α CGRP produced a significantly lower E_{\max} than h β CGRP at a number of the chimeras which involve helix 2 and its connecting loops. This resembles the differences seen between α CGRP and β CGRP at

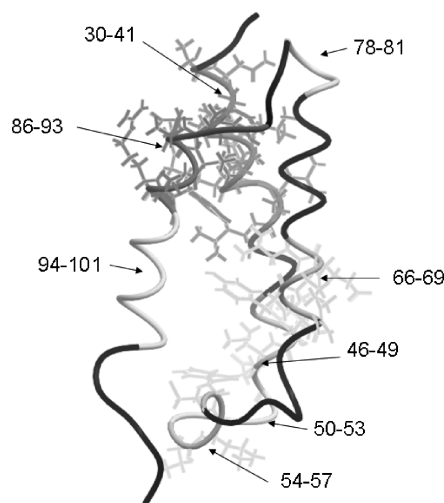


FIGURE 7: Areas of RAMP1 important for CGRP responsiveness when coexpressed with CTR. Regions identified by chimeras as showing greater than 100-fold decrease in potency for Tyr⁰-h α CGRP and h β CGRP responsiveness are shown in dark gray with residues in line form. Regions showing a 30–100-fold decrease are in light gray with residues attached. Regions showing a 10–30-fold decrease are in light gray as backbone only.

the R3_{86–89} chimera when complexed with CLR. The fact that the activity of rAmy at some chimeras was different to that of the CGRP forms is also consistent with each peptide having distinct elements to their binding pockets.

CONCLUSION

RAMPs 1 and 3 contain discrete domains, albeit with shared functions at the boundaries which mediate interactions with CLR and, less robustly, with CTR. Helix 1 is important for the overall folding of the molecule. The face formed from helices 2 and 3, together with their associated loops, serves a dual role both in recognizing CLR and binding ligands. The CLR binding site seems to be at the membrane-facing end of this face. Residues here not only bind CLR but also change its conformation, to allow ligand binding. The N-terminal end of helix 3 and especially the loop connecting it to helix 2 are of importance for ligand recognition and discrimination. This relative position of this loop between RAMPs, perhaps orientated by the sequences which flank it in helices 2 and 3, may be a key contributor to the pharmacological phenotypes of RAMP/CLR complexes.

SUPPORTING INFORMATION AVAILABLE

Figures S1 and S2 showing the stability of the models of RAMP1 and RAMP3. This material is available free of charge via the Internet at <http://pubs.acs.org>.

REFERENCES

- Hay, D. L., Poyner, D. R., and Sexton, P. M. (2006) GPCR modulation by RAMPs. *Pharmacol. Ther.* 109, 173–197.
- McLatchie, L. M., Fraser, N. J., Main, M. J., Wise, A., Brown, J., Thompson, N., Solari, R., Lee, M. G., and Foord, S. M. (1998) RAMPs regulate the transport and ligand specificity of the calcitonin-receptor-like receptor. *Nature* 393, 333–339.
- Poyner, D. R., Sexton, P. M., Marshall, I., Smith, D. M., Quirion, R., Born, W., Muff, R., Fischer, J. A., and Foord, S. M. (2002) International Union of Pharmacology. XXXII. The mammalian calcitonin gene-related peptides, adrenomedullin, amylin, and calcitonin receptors. *Pharmacol. Rev.* 54, 233–246.
- Christopoulos, A., Christopoulos, G., Morfís, M., Udawela, M., Laburthe, M., Couvineau, A., Kuwasako, K., Tilakaratne, N., and

- Sexton, P. M. (2003) Novel receptor partners and function of receptor activity-modifying proteins. *J. Biol. Chem.* 278, 3293–3297.
5. Muff, R., Buhlmann, N., Fischer, J. A., and Born, W. (1999) An amylin receptor is revealed following co-transfection of a calcitonin receptor with receptor activity modifying proteins-1 or -3. *Endocrinology* 140, 2924–2927.
6. Christopoulos, G., Perry, K. J., Morfis, M., Tilakaratne, N., Gao, Y., Fraser, N. J., Main, M. J., Foord, S. M., and Sexton, P. M. (1999) Multiple amylin receptors arise from receptor activity-modifying protein interaction with the calcitonin receptor gene product. *Mol. Pharmacol.* 56, 235–242.
7. Hay, D. L., Christopoulos, G., Christopoulos, A., Poyner, D. R., and Sexton, P. M. (2005) Pharmacological discrimination of calcitonin receptor: receptor activity-modifying protein complexes. *Mol. Pharmacol.* 67, 1655–1665.
8. Kuwasako, K., Kitamura, K., Ito, K., Uemura, T., Yanagita, Y., Kato, J., Sakata, T., and Eto, T. (2001) The seven amino acids of human RAMP2 (86) and RAMP3 (59) are critical for agonist binding to human adrenomedullin receptors. *J. Biol. Chem.* 276, 49459–49465.
9. Kuwasako, K., Kitamura, K., Nagoshi, Y., Cao, Y. N., and Eto, T. (2003) Identification of the human receptor activity-modifying protein 1 domains responsible for agonist binding specificity. *J. Biol. Chem.* 278, 22623–22630.
10. Kusano, S., Kukimoto-Niino, M., Akasaka, R., Toyama, M., Terada, T., Shirouzu, M., Shindo, T., and Yokoyama, S. (2008) Crystal structure of the human receptor activity-modifying protein 1 extracellular domain. *Protein Sci.* 17, 1907–1914.
11. Simms, J., Hay, D. L., Bailey, R. J., Konycheva, G., Bailey, G., Wheatley, M., and Poyner, D. R. (2009) Structure-function analysis of RAMP1 by alanine mutagenesis. *Biochemistry* 48, 198–205.
12. Mallee, J. J., Salvatore, C. A., LeBourdelle, B., Oliver, K. R., Longmore, J., Koblan, K. S., and Kane, S. A. (2002) Receptor activity-modifying protein 1 determines the species selectivity of non-peptide CGRP receptor antagonists. *J. Biol. Chem.* 277, 14294–14298.
13. Hay, D. L., Christopoulos, G., Christopoulos, A., and Sexton, P. M. (2006) Determinants of 1-piperidinecarboxamide, N-[2-[[5-amino-1-[[4-(4-pyridinyl)-1-piperazinyl]carbonyl]pentyl]amino]-1-(3,5-dibromo-4-hydroxyphenyl)methyl]-2-oxoethyl]-4-(1,4-dihydro-2-oxo-3(2H)-quinazolinyl) (BIBN4096BS) affinity for calcitonin gene-related peptide and amylin receptors—the role of receptor activity modifying protein 1. *Mol. Pharmacol.* 70, 1984–1991.
14. Qi, T., Christopoulos, G., Bailey, R. J., Christopoulos, A., Sexton, P. M., and Hay, D. L. (2008) Identification of N-terminal receptor activity-modifying protein residues important for calcitonin gene-related peptide, adrenomedullin, and amylin receptor function. *Mol. Pharmacol.* 74, 1059–1071.
15. Kuwasako, K., Kitamura, K., Onitsuka, H., Uemura, T., Nagoshi, Y., Kato, J., and Eto, T. (2002) Rat RAMP domains involved in adrenomedullin binding specificity. *FEBS Lett.* 519, 113–116.
16. Kuwasako, K., Kitamura, K., Nagata, S., and Kato, J. (2008) Functions of the extracellular histidine residues of receptor activity-modifying proteins vary within adrenomedullin receptors. *Biochem. Biophys. Res. Commun.* 377, 109–113.
17. Pham, V., Wade, J. D., Purdue, B. W., and Sexton, P. M. (2004) Spatial proximity between a photolabile residue in position 19 of salmon calcitonin and the amino terminus of the human calcitonin receptor. *J. Biol. Chem.* 279, 6720–6729.
18. Bailey, R. J., and Hay, D. L. (2006) Pharmacology of the human CGRP1 receptor in Cos 7 cells. *Peptides* 27, 1367–1375.
19. Bailey, R. J., and Hay, D. L. (2007) Agonist-dependent consequences of proline to alanine substitution in the transmembrane helices of the calcitonin receptor. *Br. J. Pharmacol.* 151, 678–687.
20. Wang, J. C. P., and Kollman, P. A. (2000) How well does a restrained electrostatic potential (RESP) model perform in calculating conformational energies of organic and biological molecules? *J. Comput. Chem.* 21, 1049–1074.
21. Case, D. A., Cheatham, T. E., Darden, T., Gohlke, H., Luo, R., Merz, K. M., Onufriev, A., Simmerling, C., Wang, B., and Woods, R. J. (2005) The Amber biomolecular simulation programs. *J. Comput. Chem.* 26, 1668–1688.
22. Jorgensen, W. L., Chandrasekhar, J., Madura, J. D., Impey, R. W., and Klein, M. L. (1983) Comparison of simple potential functions for simulating liquid water. *J. Chem. Phys.* 79, 926–935.
23. Humphrey, W., Dalke, A., and Schulten, K. (1996) VMD—Visual Molecular Dynamics. *J. Mol. Graphics* 14, 33–38.
24. Bailey, R. J., Bradley, J. W., Poyner, D. R., Rathbone, D. L., and Hay, D. L. (2009) Functional characterization of two human receptor activity-modifying protein 3 variants. *Peptides* (in press).